

Investigations to increase the removal rate during plasma electrolytic polishing for post-processing

Paul Geßner · Daniel Landenberger · Jörg Bagdahn

https://doi.org/10.58134/fh-aachen-rte_2025_006

Abstract

Advances in additive manufacturing have made it possible to produce complex components that are often not economically viable using conventional production methods. In order to improve the surface quality of additively manufactured components, machining or ablative post-processing methods are often required. Plasma electrolytic polishing is a particularly promising process when low roughness values are required or a high degree of gloss is desired for components. In contrast to conventional electropolishing, which often uses highly concentrated acids, plasma electrolytic polishing usually uses environmentally friendly salt solutions. In this work, basic removal mechanisms of plasma polishing were investigated, in particular the influence of gas flow and component orientation in the electrolyte on material removal. Experiments with different sample geometries showed that the orientation of the samples in the electrolyte has a significant influence on the polishing result.

The greatest roughness reduction was achieved with vertical specimen alignment, as the gas flow along the surface enhances removal. Additionally, experiments on specimen with different cavity depths revealed that gas accumulation in the cavities negatively affects plasma formation and thus material removal. The work further demonstrates that by flushing electrolyte flowing gas over the specimen, gas accumulation can be minimized and removal significantly increased.

Keywords Plasma electrolytic Polishing · post-processing

1. Introduction / Fundamentals of Plasma Polishing

Workpieces with complex geometries, such as undercuts or hollows, can often only be manufactured using additive methods. The workpieces produced by this method usually cannot be used without post-processing, as the achievable accuracy and surface quality, for example, are not sufficient for fits. The higher surface roughness compared to conventionally manufactured components requires post-processing for applications in medical technology [KRO19], for example. One possibility for post-processing is plasma electrolytic polishing.

In plasma electrolytic polishing, which is classified as electrochemical surface removal according to DIN 8590 [DIN03], the workpiece is connected as an anode and positively polarized. The process is based, like electropolishing, on anodic metal dissolution, where the anode and cathode are located in an electrolyte. In contrast to classical electropolishing, which uses direct current voltages of up to approximately 40 V [HEI14], plasma polishing employs direct current voltages in the range of 180-400 V [BOE22] or 280-320 V [BOE06]. Due to the relatively high voltages, a gas-vapor envelope forms at the anode [ZEI22], in which a plasma is generated [SCH22]. The gas formation leads to a flow, the resulting gas flows upwards.

According to Adamitzki's model [NES06], the gas-vapor envelope is bounded by a virtual anode and a virtual cathode (see Figure 1). Within this envelope, a mixture

of hot vapor and a boiling, viscous coating of the anode forms. This viscous film significantly contributes to the homogeneity and stability of the plasma and influences the interactions between the charged particles and the anode. Jacquet assumes that the anode coating acts as an insulator [JAC36]. In areas with cavities, the layer thickness is greater, resulting in a higher electrical resistance.

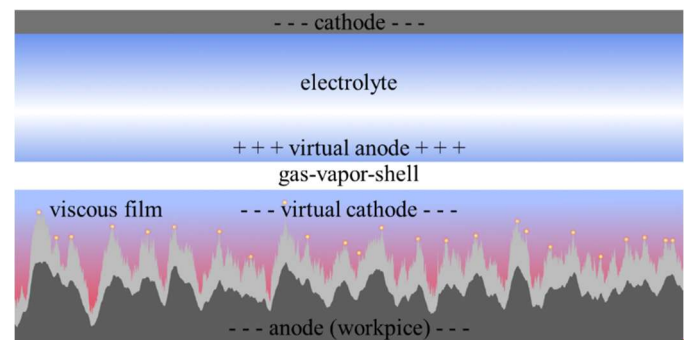


Figure 1: Model of the electrolytic cell during plasma polishing with representation of the virtual cathode (according to [NES06]) and the viscous layer (according to [ADA15]), anode with roughness profile

Plasma polishing systems typically consist of a cathodically connected polishing tank into which the workpiece is immersed (see Figure 2). Until a stable plasma forms, current peaks occur, which is why a dipping motion may be required for larger workpieces. As a result, the plasma initially forms only on limited areas of the workpiece. Non-toxic, weakly concentrated

salt solutions can be used as electrolytes, which is an advantage over classical electropolishing, where highly concentrated acids are often used. Plasma polishing systems also typically have a tank heating system, which can preheat the electrolyte around 80 °C [BOE22].

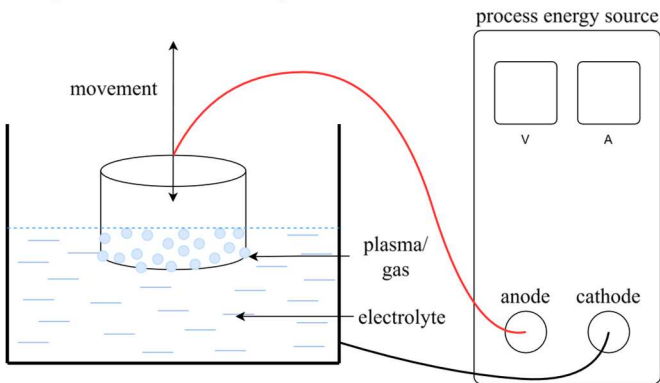


Figure 2: Schematic setup of plasma polishing

Important process parameters that influence the polishing result are:

- Process voltage
- Electrolyte temperature
- Electrolyte composition
 - Conductivity
 - pH value
 - Component orientation/electrolyte flow

Depending on the electrolyte composition and process parameters, numerous metals can be processed using plasma electrolytic polishing. The process is particularly suitable for stainless steels with a high chromium and nickel content [DEG79].

The basic suitability for the post-processing of additively manufactured workpieces was investigated using the material 1.4542 (X5CrNiCuNb16-4), which is widely used for the PBF-LB/M process. Figure 3 shows the roughness profile of an additively manufactured sample (PBF-LB/M process) made of 1.4542 (X5CrNiCuNb16-4) before and after plasma polishing. The sample was treated for 10 minutes at a process voltage of 340 V and an electrolyte temperature of 70 °C. As a result, the surface roughness is reduced from Ra 4.2 μm to Ra 1.1 μm.

Detailed plasma polishing investigations (see section 3) were carried out with the stainless steel 1.4301 (X5CrNi18-10), which has as well a high chromium and nickel content. This material is one of the most frequently [BRU05] [TRI13] used stainless steels and is used in a wide variety of industries, including additive manufacturing [STA22].

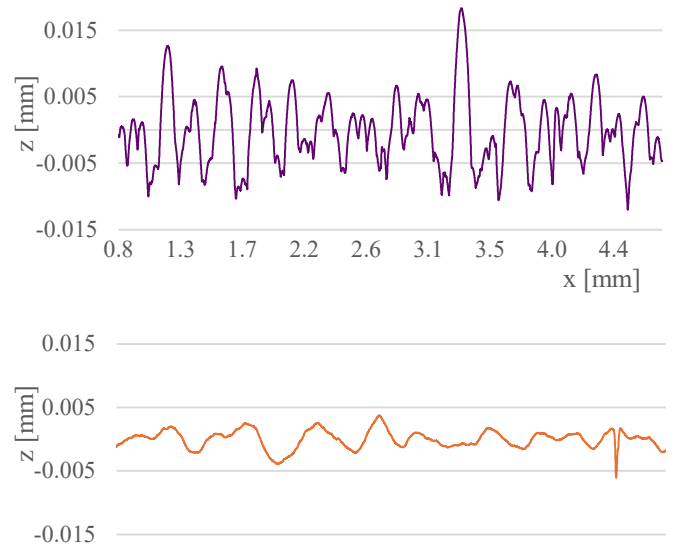


Figure 3: Roughness profiles, top: unprocessed - bottom: polished for 10 minutes

2. State of the art in the Field of Investigation

The gas formation during plasma polishing creates a flow at the workpiece. It is assumed that an optimized flow [COR20] can facilitate material removal and thus produce a smoother surface structure. It also makes it easier to treat areas that are difficult to process. A channel (1 mm high, 20 mm wide, 10 mm long) was reduced from Ra 6.53 μm to Ra 0.53 μm within 10 minutes of processing with the aid of flow [NAV22]. Material removal can also be increased by ultrasonic support [SCH22]. This shows that a flow of the electrolyte results in an increase material removal for the same machining time. Challenging are undercuts, holes and molds [SCH22]. Especially when polishing cavities, theoretical models suggest that this can be done efficiently up to a certain depth. Additionally, it is assumed that the electric field has an influence on the maximum achievable polishing depth [COR20].

According to [ZEI22], the strength of the gas layer decreases with increasing flow velocity. This leads to a lower electrical resistance of the viscous film [JAC36].

However, what has not yet been investigated is the influence of the orientation of the workpiece in the electrolyte and the possibilities for increasing the removal rate through targeted flow around the workpiece or targeted flow control.

Additionally, the polishability of cavities with downward-facing surfaces needs to be explored. In this context, it is essential to determine whether and, if so, how the plasma can effectively process these difficult-to-access areas. Ultimately, potential measures to enhance the removal performance in cavities must be explored.

3. Experimental Setup – General Conditions

The tests were carried out on a plasma polishing system from Amtopus. The electrolyte tank dimensions of the system allow workpiece dimensions of up to 300 x 500 x 300 mm³. The plasma polishing system can be used to set voltages of 340 V, 360 V, 380 V and 400 V. The maximum current of the plasma polishing machine is 150 A. The machine stops automatically if the current is higher than 150 A. This could occur if the surface of the workpiece is too large. A voltage of 340 V was selected for all the experiments presented in this article at the Anhalt University of Applied Sciences. The resulting current is essentially dependent on the workpiece properties (e.g. surface area) and the electrolyte.

For the gas flow and cavity experiments, the specimen were fabricated from stainless steel with the material number 1.4301 (X5CrNi18-10). All workpiece samples were eroded with OPS Ingersoll Gantry Eagle 400 eroding machine). The reason for this is the ability to set the target roughness of machined surfaces during erosion. This means that the comparative tests can all start with similar roughness values. If additive manufactured samples were used, a greater scatter would have to be assumed (see [CLA23]).

In order to keep the temperature as constant as possible during the process, the largest possible electrolyte volume of 300 liters was used. While polishing the electrolyte tank is cathodically polarized

The electrolyte consisted of a 5 % ammonium sulfate solution, which was adjusted to a pH value of 3.5. The electrolyte temperature was maintained at 70 °C. Figure 4 depicts the electrolyte bath, equipped with a vertically movable workpiece holder, and a workpiece.

The internationally standardized stylus method DIN EN ISO 3274 [DIN98] was chosen to determine the roughness. A scanning distance of 17.5 mm was selected for all roughness measurements. The roughness measuring device was a Mahr SD 26 stylus instrument. A Sartorius MC-1 AC210S precision balance was used to measure the mass.

During the experiments, at least seven measurements were taken at each time step, and the mean values were calculated. The standard deviations for roughness measurement and weighing are very small, therefore they were not included in the diagrams. The maximal standard deviation values are as follows:

roughness measurement orientation specimen (3.1) 0.022 μm, roughness measurement cavity specimen without flow (3.2) 0.397 μm, roughness measurement flushed cavity specimen (3.2) 0.571 μm, mass measurement 1.355 μg

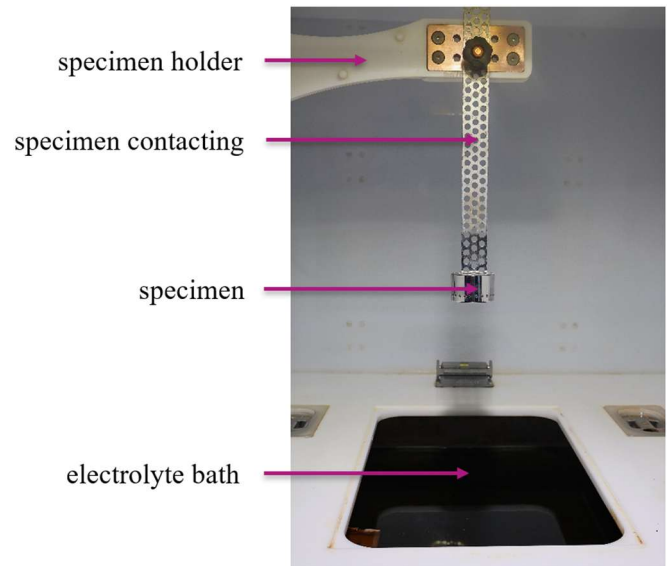


Figure 4: Experimental setup - general

3.1. Gas Flow Experiments

To facilitate a more detailed analysis of the experiments, a novel experimental setup was developed (see Figure 5). The objective was to evaluate the roughness and mass loss for a single surface. For this purpose, a workpiece holder with a flat blind hole (20 mm diameter) was fabricated. This setup enables the disassembly of the workpiece during intermediate steps, allowing the capture of mass and roughness values after different processing times. By employing a fit tolerance H7/h7 with a maximum gap width of 0.02 mm between the workpiece and the workpiece holder, plasma formation is suppressed. The back side and peripheral surface of the sample are not processed. Only the front surface is processed, and the experimental evaluation focuses on this surface. To increase the comparability of the samples, the surface to be processed was eroded. A line was marked on the sample and the roughness measurements were taken parallel to this line. The marking allowed the measured values to be recorded at the same line.

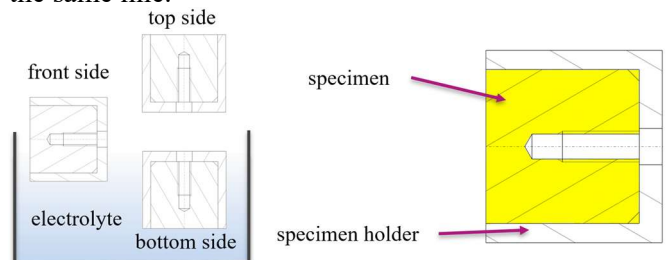


Figure 5: Orientation of the specimen in the electrolyte (left) and detailed sketch of the specimen (right)

Roughness and mass loss were measured for the orientation's bottom side, front side, and top side (see Figure 6).

The mass loss is nearly linear for all three orientations, thus validating the measurement results. Experiments

have shown that the mass removal is almost linear [RAJ17]. In contrast, the roughness reduction is not constant and tends towards a minimum value, resulting in regressive curve progressions. It is shown that the roughness reduction depends on the orientation of the specimen in the electrolyte.

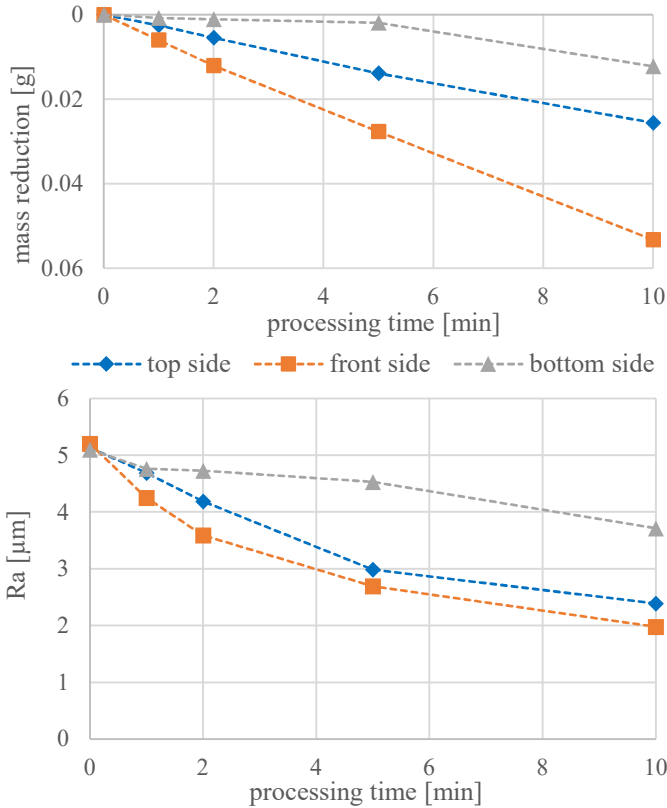


Figure 6: Dependence of the mass reduction and roughness on the machining time with different orientations of the workpiece in the electrolyte

In the last five minutes of processing time, only a minimal roughness reduction can be observed. However, since the mass removal rate remains constant, surface recession dominates. A detailed statement about the optimal processing time for economically efficient roughness reduction can be made using the time-dependent parameter of the roughness reduction rate (RRR). This involves analyzing the roughness reduction ΔR and mass removal Δm in relation to the processing time. This results in the following formula:

$$RRR(t) = \frac{\Delta R(t)}{\Delta m(t)}$$

For the experiment of gas flow using the gas flow specimen, the following trends are observed:

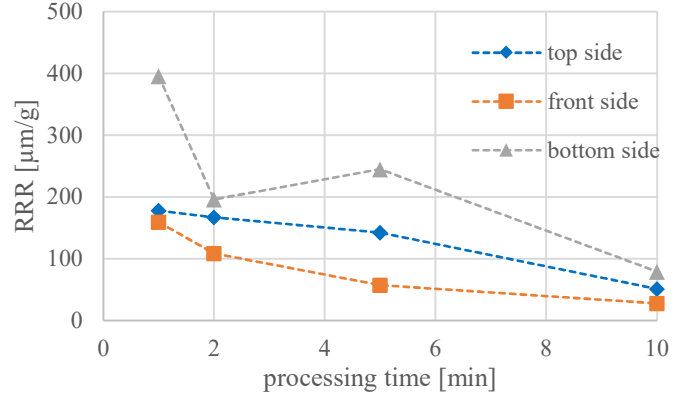


Figure 7: Roughness Reduction Rate gas flow

High values of the RRR indicate an effective roughness reduction in relation to the mass reduction (which affects the change in geometry). For functional components, where tight geometric tolerances are required, it is recommended to keep the processing time as short as possible. Since the RRR trends are material- and orientation-dependent, they must be re-determined for each specific combination.

3.2. Cavity Specimens

Furthermore, cavities of different depths, oriented downwards, should be investigated (see Figure 8). For this purpose, a special specimen holder was manufactured, which allows a disc sample with a tapped hole to be positioned at various cavity depths. Subsequently, several laterally offset roughness measurements were performed and their mean values were calculated.

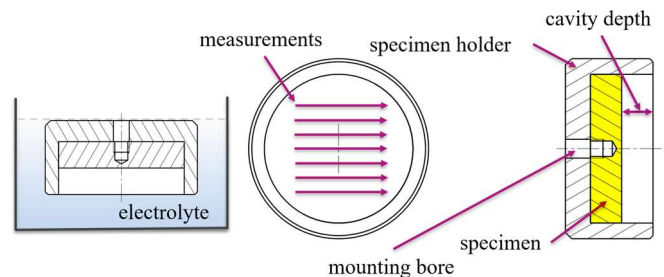


Figure 8: Cavity specimen

The specimen has a diameter of 47.5 mm. Seven measurements were conducted, each offset by 3 mm (see Figure 9). The measuring length was 17.5 mm. Their mean values were calculated from the individual measurements for the evaluation.

The cavity depth was increased step by step. The resulting cavity depths were 0 mm, 2.5 mm, 5 mm, and 10 mm (see Figure 10).

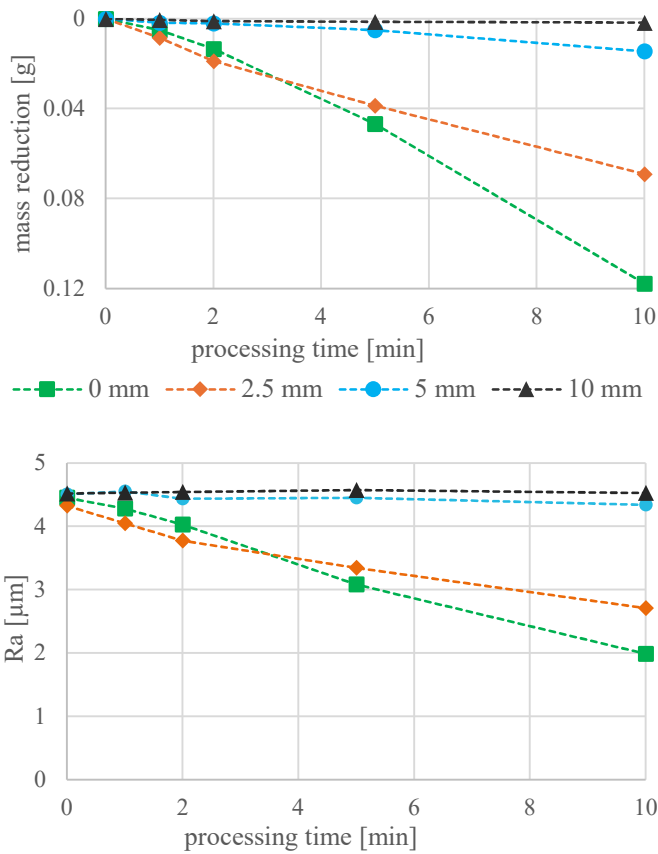


Figure 9: Dependence of the mass reduction and roughness on the machining time with different cavity depths

The curve trends indicate that the material removal decreases with increasing cavity depth. At a cavity depth of 5 mm, the removal is only minimal. It is assumed that this is due to gas formation and the associated gas accumulation in the cavity. Applying Paschen's law [KUE17], the breakdown voltage for plasma ignition can be determined. In this context, the gap distance plays a role, which increases due to the accumulation of gas in the cavity. This prevents the formation of plasma.

$$U = \frac{B \cdot p \cdot d}{\ln \frac{A \cdot p \cdot d}{\ln(1 + \frac{1}{\gamma})}}$$

U break-down voltage [V]
 p gas pressure [Pa]
 d Stroke distance [mm]
 γ 3. townsend-coefficient

A gas constant $[\frac{1}{Pa \cdot m}]$

B gas constant $[\frac{V}{Pa \cdot m}]$

From this equation, a curve is obtained for water vapor (see Figure 10). To the left of its minimum, the number of atoms for collisions is too low. On the right-hand side

of the minimum, not enough energy is gained for ionization due to the greater path length or the high pressure. [KUE17]

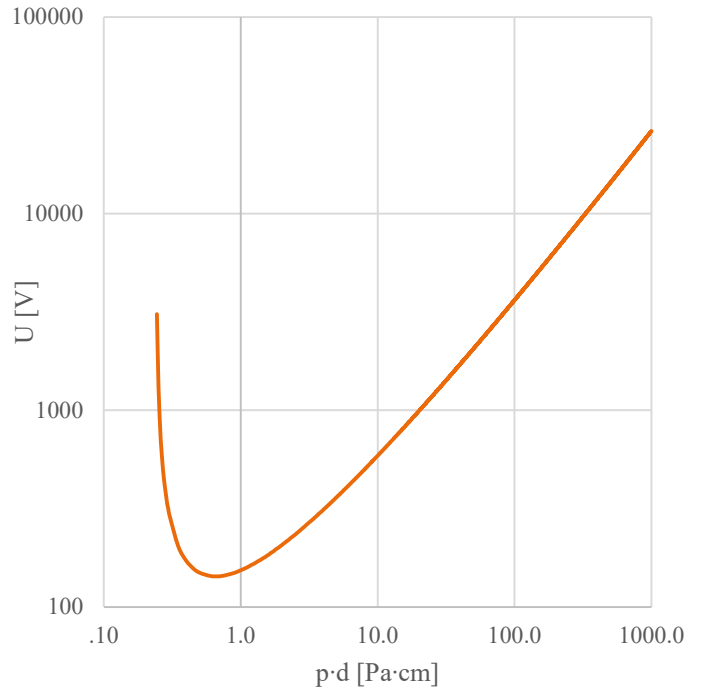


Figure 10: Paschen curve for water vapor $A=0.1(Pa \cdot cm)^{-1}$, $B=2.2 V \cdot (Pa \cdot cm)^{-1}$ and $\gamma=0.01$ [FRI08]

To minimize the impact of the stroke distance, the specimen was additionally flushed at a cavity depth of 10 mm (see Figure 11). The flushing displaces the gas in the cavity and creates a flow in this area. This results in a significantly increased material removal compared to a non-flushed cavity specimen.

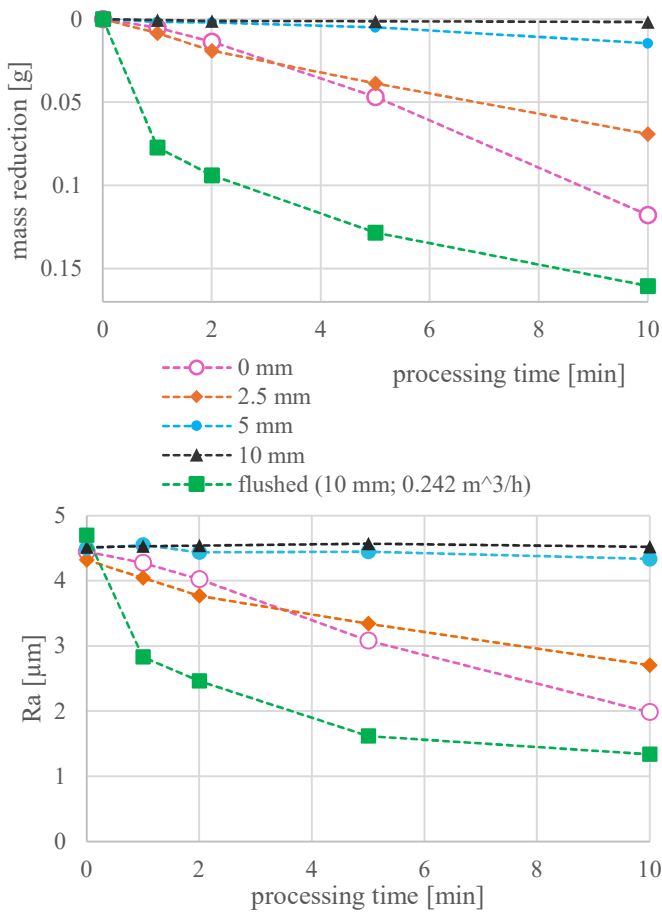


Figure 11: Dependence of the mass reduction and roughness on the machining time with different cavity depths and flushing

The erosion rate of the flushed specimen (10 mm) is significantly increased and exceeds the erosion rate at a cavity depth of 0 mm. The experimental result shows that targeted flushing can counteract the accumulation of gas bubbles and partially increase material removal. To allow the gas bubbles to escape without targeted flushing, a specimen holder with 24 x 3 mm bleeding holes was fabricated (Figure 12). Through these holes, the generated gas can escape, thereby reducing the gas film thickness. This reduces the thickness of the gas film and creates a gas flow. In addition, an influence on the viscous layer is assumed.

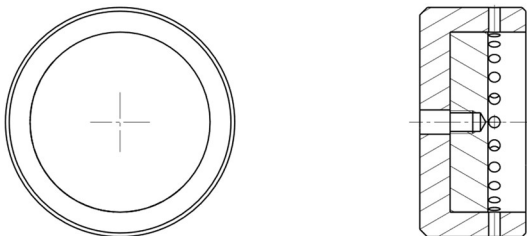


Figure 12: Specimen with bleeding holes

In the following Figure 13, it is clearly visible that surface treatment has taken place, although it is less pronounced compared to the flushed specimen.

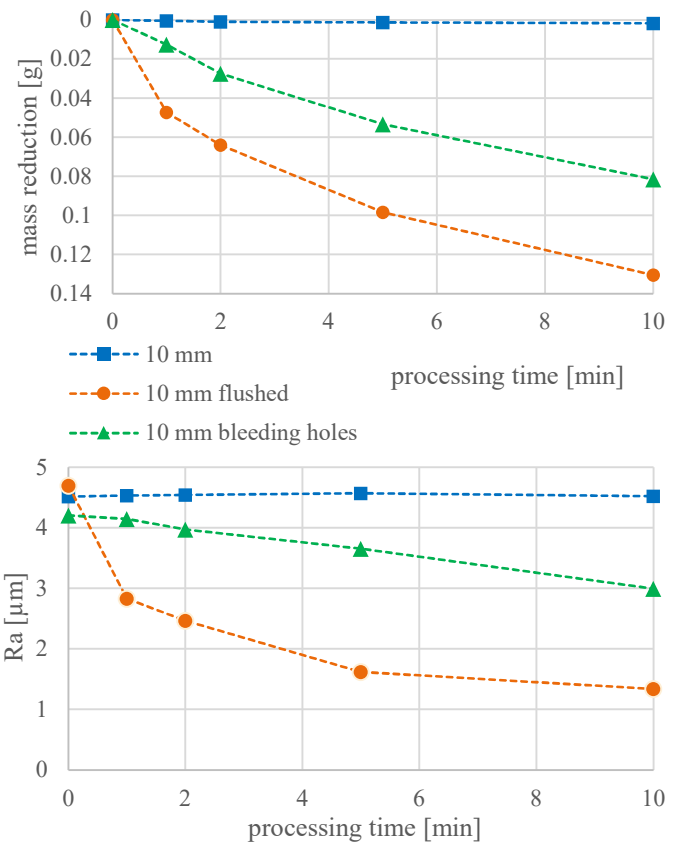


Figure 13: Dependence of the mass reduction and roughness on the machining time with different electrolyte flows against the specimen

To decouple the effect of flushing from cavity depth, two specimens were subjected to flushing with different volumetric flow rates at a cavity depth of 0 mm (Figure 14). Two distinct volumetric flow rates were utilized. Notably, the material removal rate increased with increasing volumetric flow rate. Furthermore, the minimum achievable surface roughness was reached more rapidly through flushing, whereas the material

removal rate was substantially enhanced compared to specimens without flushing.

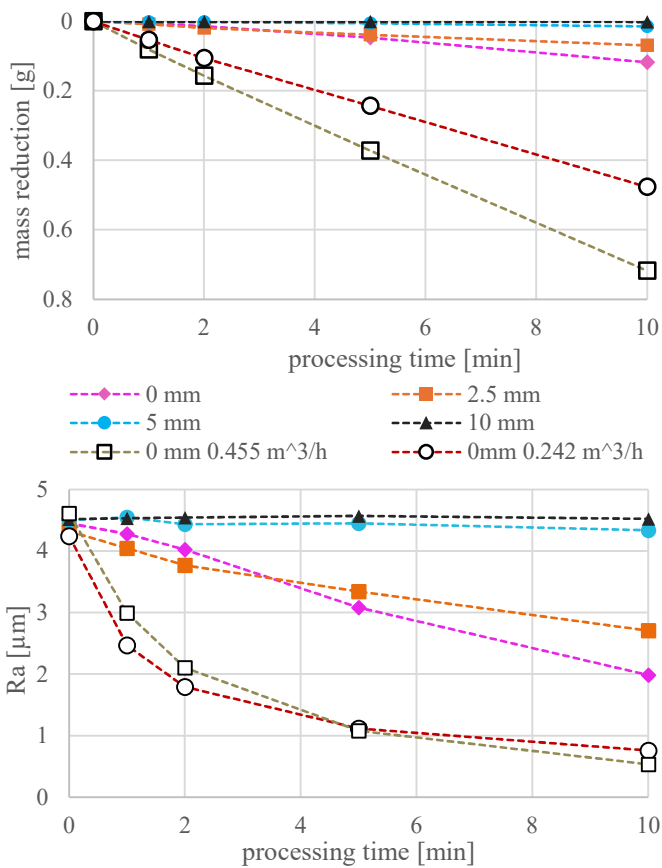


Figure 14: Diagrams of flow variation and volume flow

To contextualize the material removal, the mass removal rates per unit area are presented in the following figure. The processing time was 4 minutes in this case. The present results were compared with results from literature [BOE22]. The mass removal rates of samples without measures to enhance removal are comparable to literature values. In the reference [BOE22], high-intensity ultrasound was employed, and the sonotrode distance to the specimen was varied. The highest mass removal rate through ultrasound assistance was achieved at a distance of 3 mm, resulting in a 55 % increase. In contrast, the removal rate through flushing with a volumetric flow rate of 0.455 m³/h resulting in an increase of 800 % from 2.1 mg/cm² to 16.8 mg/cm².

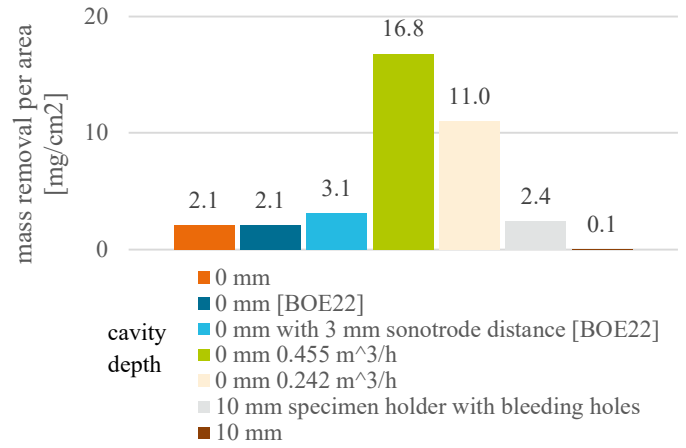


Figure 15: Comparison of material removal increases

The targeted application of electrolyte flow facilitates a substantially higher material removal rate and accelerated attainment of the desired surface finish. From a practical perspective, this implies that surfaces with stringent surface requirements can be rapidly brought to the desired roughness/gloss through flushing, leading to considerable reductions in processing times and enhanced overall efficiency.

4. Conclusion and outlook

This study explores the optimization of the plasma electrolytic polishing process to concurrently achieve high material removal rates and uniform surface finishes. A key consideration is the prevention of gas bubble accumulation, as this can substantially impact removal rates.

The results demonstrate that supplementary flushing of the electrolyte significantly enhances removal rates, highlighting the importance of ensuring effective workpiece flushing. Another critical factor is the vertical orientation of relevant surfaces to accelerate material removal. In addition to optimizing removal rates, the roughness reduction rate must also be taken into account to ensure efficient and geometry-preserving polishing.

Further research using devices for partial flushed polishing (e.g., wide-slot nozzles) offers considerable benefits for functional components, enabling more targeted material removal and reduced process times. For workpieces with cavities, it is to investigate whether increased processing voltages can improve their machinability.

It must also be investigated whether the flow influences the waviness and form deviation. The relationship between edge rounding and roughness reduction rate is also a research topic.

5. Acknowledgement

The machine used for the investigations was funded by the Federal Ministry of Education and Research (BMBF) under grant number 03WIR21IL2.

The authors express their sincere thanks to the funding program “Sachsen-Anhalt WISSENSCHAFT Forschung und Innovation (EFRE)” with the grant number 8377/1001, with the title “Plasmapolieren – Untersuchung des plasmaelektrolytischen Polierens von Funktionsbauteilen aus Einsatzstahl”. Financed from the European union and the state of Saxony Anhalt.

References

- [ADA15] Adamitzki, W.: Herstellung und Veredelung von Komponenten für centrifluidische Systeme, Elektrolytforschung für das Plasmapolieren von Komponenten für centrifluidische Systeme, Abschlussbericht, Wachstumskern Centifluid, 2015
- [BOE06] Böhm, A., Kluchert, C., Lingath, K. a. o.: Anlage und Verfahren zum Reinigen und Polieren der elektrisch leitfähigen Oberfläche eines Werkstückes sowie Verwendung des Verfahrens, DE 10 2006 016 368 B4, Deutsches Patent- und Markenamt, 2006
- [BOE22] Zeidler, H. and Böttger-Hiller, F.: Plasmaelektrolytisches Polieren Ein Überblick über angewandte Technologien und aktuelle Herausforderungen, Jahrbuch Oberflächentechnik, Eugen G. Leuze Verlag, Bad Saulgau, 2022
- [BRU05] Brüssel, B., Tildonk, M.: Merkblatt 968, Mechanische Oberflächenbehandlung nichtrostender Stähle in dekorativen Anwendungen, 1. Edition, Euro Inox, 2005
- [CLA23] Clark, C.L., Karasz, E.K., Melia, M., a.o.: Machine-to-machine variability of roughness and corrosion in additively manufactured 316L stainless steel, Journal of Manufacturing Processes, Elsevier Ltd, 2023
- [COR20] Cornelsen, M. S.: Prototypenanlage und Prozessuntersuchung zum elektrolytischen Plasmapolieren von Rohrrinnenoberflächen, Dissertation, Universität Rostock, 2020
- [DEG79] Degner, W., Böttger, H., Steinhäuser, S.: Handbuch Feinbearbeitung, VEB Verlag Technik Berlin, Berlin, 1979
- [DIN03] DIN 8590: Fertigungsverfahren Abtragen - Einordnung, Unterteilung, Begriffe. DIN Media, Berlin, 2003
- [DIN98] DIN EN ISO 3274: Oberflächenbeschaffenheit: Tastschnittverfahren Nenneigenschaften von Tastschnittgeräten, DIN Media, Berlin, 1998
- [FRI08] Fridman, A.: Plasma Chemistry, Cambridge University Press, Cambridge, 2008
- [HEI14] Heisel, U., Klocke, F., Uhlmann, E., Spur, G. (Hrsg.): Handbuch Spanen, Carl Hanser Verlag, München, 2014
- [JAC36] Jacquet, P.A.: On the anodic behavior of copper in aqueous solutions of orthophosphoric acid, article, New York, 1936
- [KRO19] Kröning, O., Schulze, H., Zeidler, H., a.o.: Das Plasma-elektrolytische Polieren von Werkstücken für den medizinischen Einsatz, Magdeburger Maschinenbautage 2019 – MAGDEBURGER INGENIEURTAGE -, conference article, Magdeburg, 2019
- [KUE17] Küchler, A.: Hochspannungstechnik Grundlagen - Technologie - Anwendung, 4th edition, Springer-Verlag GmbH, Berlin, 2017
- [NAV22] Navickaitė, K., Nestler, K., Kain, M., a.o.: Effective polishing of inner surface of additive manufactured inserts for polymer extrusion using Plasma Electrolytic Polishing, 18th Rapid Tech 3D, Erfurt, 2022
- [NES06] Nestler, K., Adamitzki, W., Unger, M., Faust, W., a.o.: Plasma Polishing of metallic surfaces – effects and models, international symposium on electrochemical machining technology, INSECT, Dresden, 2006
- [RAJ17] Rajput, A., Zeidler, H., Schubert, A.,: Analysis of voltage and current during the Plasma electrolytic Polishing of stainless steel, euspens` s 17th International Conference & Exhibition, Hannover, 2017
- [SCH22] Schulze, H., Zeidler, H., Kröning, O., Böttger-Hiller, a.o.: Process analysis of plasma-electrolytic polishing (PeP) of forming tools, International Journal of Material Forming, Springer-Verlag, 2022
- [STA22] Starecek, J., Prejda, V., Moravec, P., a.o.: Numerical investigation of the impeller blades, manufactured by metal 3D printing technology with internal structures, MM Science Journal, 2022
- [TRI13] Tritschler, M.: Vorhersage der Rückfederung beim Umformen von nichtrostendem Edelstahl, wt Werkstattstechnik, Düsseldorf, 2013
- [YER19] Yerokhin, A., Mukaeva, V., Parfenov, E., a.o.: Charge transfer mechanisms underlying Contact Glow Discharge Electrolysis, article, Elsevier Ltd., London, 2019
- [ZEI22] Zeidler, H., Böttger, T., Schröder, S., a.o.: Analysis of Plasma-Electrolytic Polishing Process Initiation, 6th CIRP Conference on Surface Integrity, Elsevier, 2022

Remark: The chatbots ChatGPT and deepL were used to optimise English-language formulations.